

Mechanical characterization device for in situ measurement of nanomechanical properties of micro/nanostructures

Utkarsha Singh, Vikas Prakash, Alexis R. Abramson, Wei Chen, Liangti Qu et al.

Citation: *Appl. Phys. Lett.* **89**, 073103 (2006); doi: 10.1063/1.2271576

View online: <http://dx.doi.org/10.1063/1.2271576>

View Table of Contents: <http://apl.aip.org/resource/1/APPLAB/v89/i7>

Published by the [American Institute of Physics](#).

Additional information on *Appl. Phys. Lett.*

Journal Homepage: <http://apl.aip.org/>

Journal Information: http://apl.aip.org/about/about_the_journal

Top downloads: http://apl.aip.org/features/most_downloaded

Information for Authors: <http://apl.aip.org/authors>

ADVERTISEMENT

**AIP**Advances

Submit Now

**Explore AIP's new
open-access journal**

- **Article-level metrics
now available**
- **Join the conversation!
Rate & comment on articles**

Mechanical characterization device for *in situ* measurement of nanomechanical properties of micro/nanostructures

Utkarsha Singh, Vikas Prakash, and Alexis R. Abramson^{a)}

Mechanical and Aerospace Engineering, Case Western Reserve University, Cleveland, Ohio 44106

Wei Chen, Liangti Qu, and Liming Dai

Chemical and Materials Engineering, University of Dayton, Dayton, Ohio 45469

(Received 20 December 2005; accepted 19 June 2006; published online 15 August 2006)

A characterization device was developed for nanomechanical testing on one-dimensional micro/nanostructures. The tool consists of a nanomanipulator, a three-plate capacitive transducer, and associated probes, and is operated inside a scanning electron microscope. The transducer independently measures force and displacement with micronewton and nanometer scale resolutions, respectively. Tensile testing of a polyaniline microfiber (diameter $\sim 1 \mu\text{m}$) demonstrated the capabilities of the system. Engineering stress versus strain curves exhibited two distinct regions with different Young's moduli. Failure at the probe-sample weld occurred at $\sim 67 \text{ MPa}$, suggesting that polyaniline microfibers exhibit a yield stress that is higher than most comparable bulk polymers.

© 2006 American Institute of Physics. [DOI: 10.1063/1.2271576]

Though several inventive experimental techniques have been recently proposed and implemented to obtain the nanomechanical behavior of one-dimensional nanostructures, complexities such as nanostructure positioning, alignment, attachment to probes/grips, and achieving superior force and displacement resolutions have complicated these characterization efforts. Early attempts in nanomechanical characterization were essentially indirect methods and involved the study of vibrations/oscillations in nanostructures, induced by thermal vibrations¹ and/or by application of an electric field,² within a transmission electron microscope (TEM). Atomic force microscopy (AFM) and other scanning probe microscopy methods have also been utilized to conduct nanomechanical testing;³ these techniques were further advanced by Yu *et al.*⁴ to develop a piezoactuated nanomanipulator with AFM probe tips inside a scanning electron microscopy (SEM) chamber. More recently, Zhu *et al.*⁵ and Haque and Saif⁶ have developed micro-electro-mechanical sensor-based testing devices for *in situ* mechanical testing of nanostructures within a SEM or TEM.

This letter reports on the development of a nanomechanical test and characterization device for one-dimensional nanostructures which in contrast to some of the previously developed methods, circumvents many of the complexities often present with nanoscale characterization while achieving reliable and accurate results. The device features independent measurement of both force and displacement histories in the test sample with micronewton force and nanometer displacement resolutions. Moreover, the tool is well suited for *in situ* testing within a SEM, which permits continuous high-resolution imaging during nanomechanical straining. As schematically shown in Fig. 1, the device comprises of two main parts: (a) a three-plate capacitive transducer (Hysitron, Inc.) that doubles both as an actuator and a force sensor; and (b) a nanomanipulator (Kleindiek MM3A) that facilitates transportation and positioning of the nanoscale structures with nanoprecision. The capacitive transducer

is commercially available and is more commonly used in nanoindentation and surface scratching studies in conjunction with a Veeco Dimension 3100 AFM (i.e., the Hysitron Triboscope). However, in the present study it has been alternatively contrived to characterize the nanomechanical tensile behavior in individual nanostructures. To conduct the experiments the two ends of the nanowire specimen are individually attached to probe tips on the nanomanipulator and the transducer, using nanopositioning and ion-beam induced deposition (IBID). The process involves precision metering of predetermined organometallic gas precursors into the SEM chamber (FEI XT Nova nanoLab 200) via a micro-delivery gas-injection system (FEI FP 3400/30), where a high intensity electron or ion beam is used to form relatively high strength deposits at its focal point. The electron-beam is typically used for smaller diameter ($< 1 \mu\text{m}$) specimens; the ion-beam has been found to be more effective in micro-welding the larger diameter fiber specimens. The capabilities of the testing device are illustrated by presenting results of nanomechanical characterization of $\sim 1 \mu\text{m}$ diameter polyaniline fibers synthesized by using an electro-spinning process.⁷

Figure 1 illustrates the nanomanipulator and the three-plate capacitive transducer mounted onto the *x-y-z* stage of

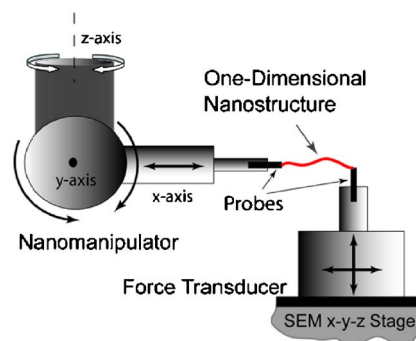


FIG. 1. (Color online) Schematic of the nanomechanical characterization device showing the magnified view of the sample between two probes and the available degrees of freedom.

^{a)}Electronic mail: vikas.prakash@case.edu

the SEM. The nanomanipulator has three degrees of freedom: linear motion with a resolution of 1 nm in the direction along the axis of the probe (x -axis), and rotational motion about the y and z axes. A commercially available platinum iridium probe (Micromanipulator Company, Inc., 7X), with a tip radius of 100 nm, was employed at the end of the nanomanipulator. A custom made actuator probe made of a commercially available aluminum alloy and having a tip radius of $250\ \mu\text{m}$ is screwed directly on to the force transducer; the probe tip has two degrees of freedom—one along the x axis (specimen loading direction) and the other in the z axis, which is also the vertical axis of the actuator probe. The transducer works on the principle of differential capacitance and serves as a combined actuator and sensor unit. As per the manufacturer's specification (and also in consideration of the noise effects), in the z direction, the transducer can apply a maximum force of 10 mN with a resolution of 100 nN and a maximum displacement of $5\ \mu\text{m}$ with a resolution of 0.2 nm. In the x direction, accounting for the noise floor, the maximum force the transducer can apply is limited to 2 mN with a resolution of $10\ \mu\text{N}$, while the maximum displacement is limited to $\pm 7.5\ \mu\text{m}$ with a resolution of 10 nm.

In the experiments described herein, in order to conduct the nanomechanical tensile experiments on individual fibers, polyaniline microfibers were initially isolated from the non-woven electrospun mat by employing the Kleindiek nanomanipulator within the SEM. Scanning electron microscopy revealed the mean diameter of these isolated polyaniline fibers to vary between 1 and $1.2\ \mu\text{m}$. Next, one end of the fiber sample was welded to the nanomanipulator probe tip by depositing platinum using the IBID process. The microfiber specimen was then pulled from the substrate and cut to a length of $\sim 199\ \mu\text{m}$ using the ion beam. The isolated polyaniline microfiber was then transported to the actuator probe, where it was first aligned parallel to the loading axis and then welded onto the actuator probe tip using the IBID process. The specimen was then manipulated to remove any slack.

For the experiment to proceed, the nanomanipulator was held stationary while the transducer was programmed to be stretched to a maximum displacement of $5\ \mu\text{m}$ at a rate of $0.5\ \mu\text{m/s}$. After a dwell time of 10 s, the microfiber was then unloaded to its original position. During the loading and unloading processes, the force was sensed by the three-plate capacitive transducer. While every effort was taken to visually align the nanofiber axially, any misalignment results in a forces in both the lateral and axial directions. Nonetheless, since the transducer provides simultaneous force and displacement measurements in both the lateral and the axial directions, elementary geometry was employed to determine the axially resolved force and displacement history. Using these force and displacement histories along with the knowledge of the initial diameter of the microfiber, engineering stress versus engineering strain curves were obtained.

Figure 2 illustrates the behavior for the $\sim 1\ \mu\text{m}$ diameter polyaniline fiber that was displaced $2\ \mu\text{m}$, held for 10 s, and then unloaded to its initial position (Test 1). The open circles denote the loading segment, while the filled triangles and the open squares represent the holding and the unloading segments. It is to be noted that that the loading and unloading paths in the engineering stress and strain space for the electrospun polyaniline fibers are not coincident. Additionally, there is a fairly gradual slope associated with the early loading segment of the stress-strain curve when compared to

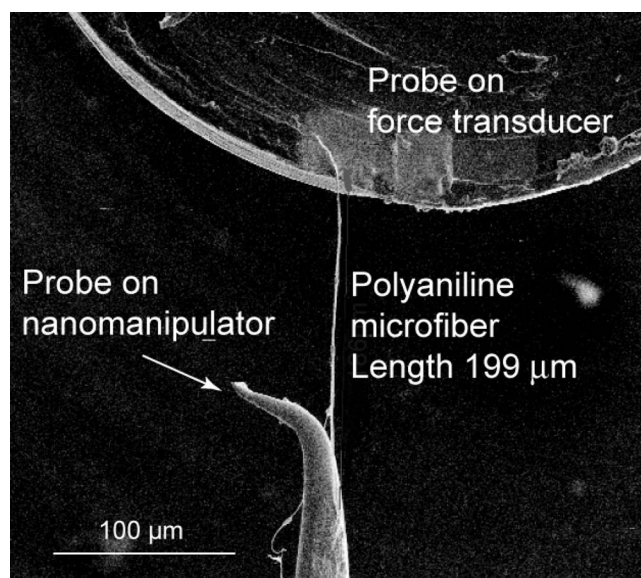


FIG. 2. A high resolution SEM picture of the polyaniline microfiber specimen microwelded to the probe tips of the nanotensilemeter prior to the tensile test.

larger levels of strain, indicating the stiffness of the polyaniline microfibers is much lower at small levels of strain, but increases quickly as higher levels of axial strain are introduced. This unusual material response may be indicative of the stress and strain states in polyaniline that are associated with the stretching and reorientation of the secondary (weak van der Waals) bonds between the polymer chains during the very early part of the deformation, followed by a continuous increase in stiffness that is representative of the load carried by a more aligned molecular chain structure. This varying stiffness behavior is also observed during the unloading segment of the stress-strain curve when the stress falls quickly with strain (up to ~ 0.006), and then the decrease becomes more gradual. Such molecular realignment processes are undoubtedly also present during deformation of bulk polymer specimens; however, to the best of our knowledge, no existing measurements of force and displacement on bulk polymer systems have been made with the same resolution and accuracy as the current measurements, and thus have not been reported in the literature. Moreover, it is interesting to note that this varying stiffness behavior is also observed during the unloading segment of the stress-strain curve. The Young's moduli, associated with the loading and the unloading segments in the low strain regime (with strains less than ~ 0.006) are estimated to be 0.38 GPa and 0.45 GPa, respectively. The Young's moduli at the larger strains (i.e., $> \sim 0.006$) are difficult to estimate from the data in Fig. 3, and are obtained from Test 2, described next.

A second tensile test (Test 2) was then conducted on the same specimen, but the transducer was actuated to its maximum displacement of $5\ \mu\text{m}$ at a rate of $0.5\ \mu\text{m/s}$. The resulting engineering stress versus strain curve is shown in Fig. 4, as indicated by the filled squares. The results from the previous experiment (Test 1) are also shown on the graph for comparison and can be more clearly seen in the inset. The most striking feature of the experimental results is that the stress-strain behavior of the polyaniline microfiber is obtained up to strains of 0.022, after which a sharp fall in stress is observed. This precipitous drop in stress is understood to

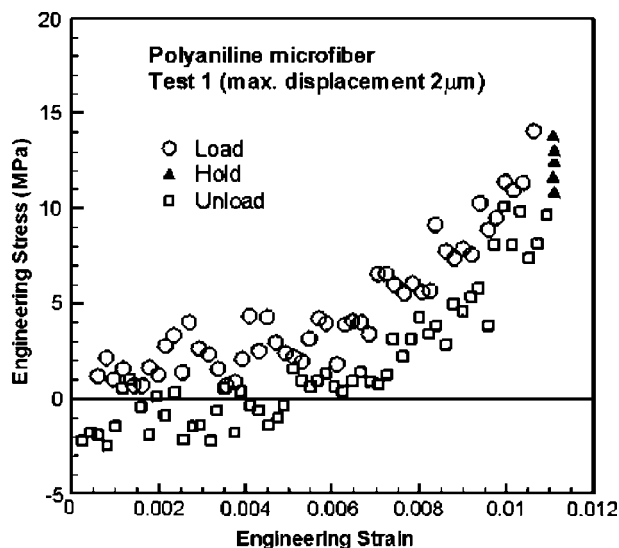


FIG. 3. Engineering stress-strain curve for an $\sim 1 \mu\text{m}$ diameter polyaniline microfiber (Test 1) showing the load (open circles), hold (filled triangles), and the unload (open squares) segments; the initial specimen length was $\sim 200 \mu\text{m}$, the applied displacement rate was $0.5 \mu\text{m/s}$, and the maximum displacement was $2 \mu\text{m}$. The hold time was 10 s.

correspond to failure of the specimen near the fiber-probe weld junction at the actuator probe end. This premature failure is in part due to the IBID process that was used for nanowelding, which perhaps led to degradation of the mechanical strength of the polyaniline fiber near the weld, and partly due to the misalignment of the sample with the loading axis, which is expected to induce additional multiaxial deformation modes (bending and torsion) in the sample, especially near the clamp. Nevertheless, the experiment indicates that the strength of polyaniline microfibers is at least $\sim 67 \text{ MPa}$, which is much larger than the yield strength reported for most polymeric materials in their bulk state under quasistatic deformation conditions. Moreover, the stress versus strain curve in Fig. 3 depicts two distinct regions, which were also observed in Fig. 2; these regions likely correspond to the initial stretching and/or reorientation of the polymer chains followed by loading of the more aligned structure. The slope of the stress-strain curve in the latter strain regime (strain $\sim 0.006\text{--}0.02$) is estimated to be 5.9 GPa . Additional

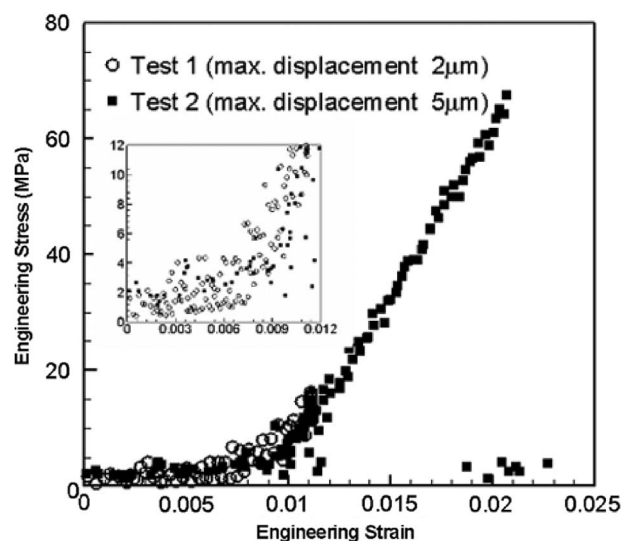


FIG. 4. Engineering stress and strain for Test 1 (open circles) and Test 2 (filled squares); the latter experiment involved loading the sample to $5 \mu\text{m}$; failure at the probe-sample weld occurred prior to reaching this maximum displacement; the inset magnifies the data up to 12 MPa .

in situ testing of micron and nanosized polyaniline fibers is currently being pursued and will be reported in future publications.

This research conducted in the present study is supported by the National Science Foundation under Award No. CTS 0438389, and equipment Grant Nos. CMS 0521364 and CMS 0326832.

¹M. M. J. Treacy, T. W. Ebbesen, and J. M. Gibson, *Nature (London)* **381**, 678 (1996).

²P. Poncharal, Z. L. Wang, D. Ugarte, and W. A. de Heer, *Science* **283**, 1513 (1999).

³W. Shen, B. Jiang, B. S. Han, and S. S. Xie, *Phys. Rev. Lett.* **84**, 3634 (2000).

⁴M. F. Yu, O. Lourie, M. J. Dyer, K. Moloni, T. F. Kelly, and R. S. Ruoff, *Science* **287**, 637 (2000).

⁵Y. Zhu, N. Moldovan, and H. D. Espinosa, *Appl. Phys. Lett.* **86**, 013506 (2005).

⁶M. A. Haque and M. T. A. Saif, *Sens. Actuators B* **97-98**, 239 (2002).

⁷L. Dai and D. H. Reneker, in *Nanowires and Nanobelts: Materials, Properties and Devices*, edited by Z. L. Wang (Kluwer Academic, Dordrecht, 2003), Vol. 2, p. 375.